Modeling of Torque Vectoring Drives for Electric Vehicles: a Case Study

Franciscus L.J. van der Linden Jakub Tobolář

German Aerospace Center (DLR), Institute of System Dynamics and Control, 82234 Wessling, Germany
{Franciscus.vanderLinden,Jakub.Tobolar}@dlr.de

Abstract

This paper shows some aspects of the implementation of a gear model with losses, nonlinear elasticity and forcing errors in the Modelica language utilizing concept of replaceable functions. Using such gear model for a torque vectoring drive modeling, a case study about a powertrain dynamic behavior in a simplified vehicle model is carried out. The total vehicle model is analyzed in several detail stages of the powertrain reaching from a fixed efficiency with constant spring stiffness to a model using nonlinear losses and nonlinear tooth stiffness. Subsequently, the simulation results of such levels of modeling detail proving tendency to drive line oscillation are presented and discussed.

Torque Vectoring Drive, Gearing, Vehicle Dynamics

1 Introduction

To design the gearing solution for an electrical vehicle, different gear topographies are typically analyzed utilizing computer simulations in an early design stage. To perform such studies efficiently, it is important that the gearing topographies can easily be designed and integrated into the vehicle models which are used for maneuverability tests assessing the driving quality.

A solution enabling such gear topography design and vehicle integration was introduced recently by (van der Linden, 2015). To prove the usability of that concept also for more complex gearing topographies, an electric vehicle powertrain configuration with controlled torque vectoring device was chosen in this paper – a future-oriented solution particularly suitable to actively influence the dynamic behavior of the vehicle, such as using active yaw rate control. Such a torque vectoring drive (TVD) configuration is used e. g. in experimental cars like the VISIO.M (Gwinner et al., 2014) and allows for very high vectoring torques with a small electric motor.

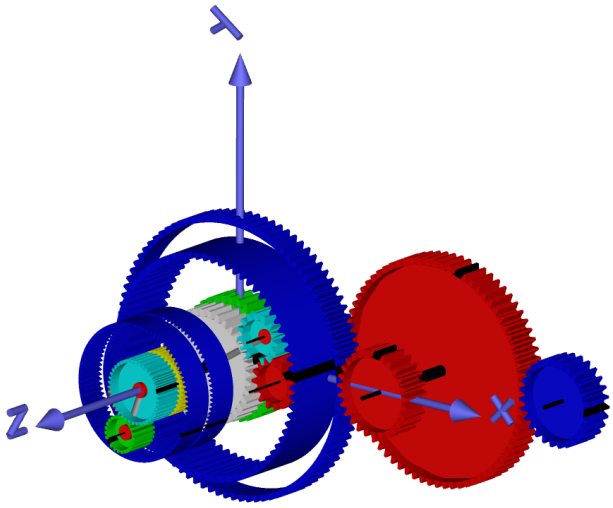

Figure 1. Torque vectoring drive consisting of a differential, superimposing unit and spur gear train. Note that only single planets are shown for simplification of the calculations.

A graphical overview of the gearing solution is shown in Figure 1.

After giving an overview of some implementation aspects of the method in Section 2, the present study will continue with a TVD model decription in Section 3. Here, a gear with constant elasticity and constant efficiency will be first introduced as a reference model. For further investigations, the model complexity will be successively increased with different loss models as well as nonlinear elasticity and backlash in the gearing. Utilizing a simple vehicle model, briefly referred in Section 4, the simulation results will be discussed in detail in Section 5.

2 Gear model description

The gear models used in this analysis base on previous work which consisted of the simulation of elastic ideal gears (van der Linden, 2012). These models have been extended with various loss models and elasticity models according to (van der Linden,

2015). An overview of the forces and torques calculated in this publication are shown in Figure 2. The forces and torques (F_{xA}, F_{yA}, τ_A, F_{xB}, F_{yB} and τ_B) in this Figure are calculated using the integral of the forces of a complete cycle of the meshing tooth. By supplying also an internal gear force element, epicyclic gears can be modeled as well. Since the derivation of all the theory goes beyond the scope of this paper, only brief outline is given in the following sections. For a detailed description, please refer to the abovementioned paper. Since the derived model of gear teeth contact is purely planar, it is implemented using the PlanarMechanics toolbox (Zimmer, 2012). This allows the use of standard planar parts and enables a good transferability of forces and torques into the 3D world

2.1 Friction force implementation

Since in gear dynamics different friction models are often used, a decision was made to implement the friction using a replaceable function structure.

The friction is implemented using a state machine to be able to handle friction during the `Forward`, `Backward` and `Stuck` mode. To switch between these modes, two transition modes are used: `StartForw` and `StartBackw`. A tearing variable `sa` is used in the Stuck mode to calculate the forces to keep the model stuck. This approach is similar to the friction implementation of (Otter et al., 1999). The gear friction force F_t is calculated using specialized functions based on e. g. gear meshing speed, operational mode of the gear contact, contact angle and the radii of the gear wheels.

The concept of replaceable functions allows for a quick selection between the different friction models: no friction, viscous friction, specified efficiency, Coulomb friction, friction according to the DIN 3990 specifications (DIN 3990 Teil 4, 1987) and a friction implementation from Niemann and Winter (1989). The DIN 3990 friction and the friction to Niemann and Winter both define the friction as a function of the speed and loading of the gear.

Furthermore, a continuous friction model which is not based on a state machine is implemented. This implementation uses a regularized friction model to smooth the discontinuity of the gear friction. It is implemented using

$$F_t = \mu |F_n| \tanh \frac{|v_{mesh}|}{v_{mesh,0}}. \quad (1)$$

In this equation, v_{mesh} is the relative speed of the gears at the meshing point and $v_{mesh,0}$ the characteristic meshing speed which is chosen small compared to the nominal meshing speed. Using this regularization, event chattering of gear systems with many gear contacts can be avoided. However, it must be noted that in this case no stiction can take place, as the friction is zero at zero speed.

In this paper, a fixed friction coefficient will be used as this method is heavily used in the design of gear transmissions for powertrain analysis, together with the friction implementation to the DIN 3990 norm due to a good match with measured friction results in a previous publication (van der Linden, 2015).

2.2 Elasticity implementation

Similar to the variability of friction methods used in the modeling of gears, also the gear elasticity is described in many ways. In most cases, a nonlinear relation between normal forces F_n and deformation of the gear at contact is present. To incorporate the different stiffness models known from literature, also the elasticity is implemented using another set of replaceable functions. These functions calculate the normal contact force F_n from multiple model inputs like the mesh deformation and speed, gear radii, thickness of the wheels and wheel positions. The position of the gear wheels makes it possible to include a position dependent gear stiffness which can be used to simulate the effect of meshing teeth or the effect of a damaged tooth.

2.3 Forcing error implementation

To simulate forcing errors like misalignment of the gear wheels, manufacturing errors or damaged tooth, a position dependent forcing error is added to the overall gear deformation. In Figure 3, the deformation between the gears is given by $\Delta_{AB} = \Delta_{AB,0} + \Delta_{AB,e}$. In this equation, $\Delta_{AB,e}$ is the elastic deformation of the gear contact as discussed in Section 2.2. Adding the forcing distance $\Delta_{AB,0}$ gives the total gear deformation.

Also in this case, replaceable functions are used to implement several cases: a forcing error defined by the misalignments of the gears, a forcing error defined by a Fourier-series and a table-based interpolation. All these methods define the forcing error as a function of the position of each gear wheel.

2.4 Graphical representation of gears

The graphical representation of the gears is an important way to check proper geometry of the gear. Therefore, visualizers from `Modelica.Mechanics.MultiBody.Visualizers` are used to visualize the gear wheels. The results of such exemplary 3D representations can be seen in Figure 1 and Figure 5. The parameters needed for the visualization, such as gear radius or thickness, are directly taken from the gear model parameters.

DOI 10.3384/ecp15118151

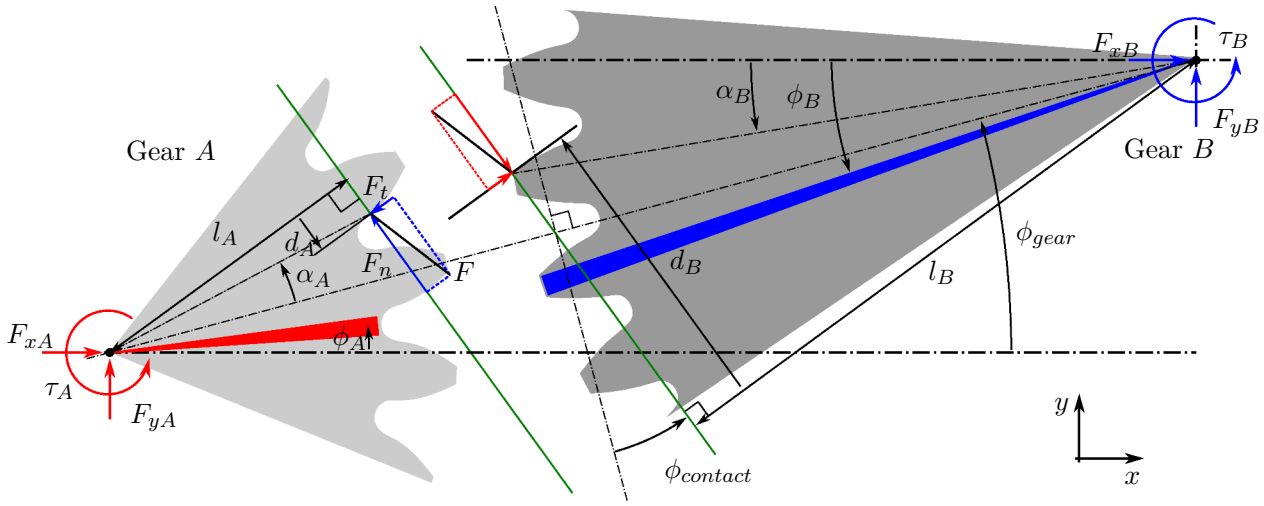

Figure 2. Free body diagram of two involute gears. In the figure $\omega_A < 0$ and Gear A drives Gear B.

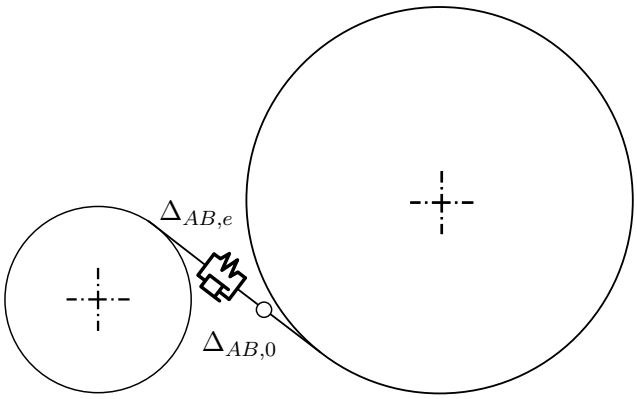

Figure 3. Forcing error excitation using a position dependent forcing distance $\Delta_{AB,0}$

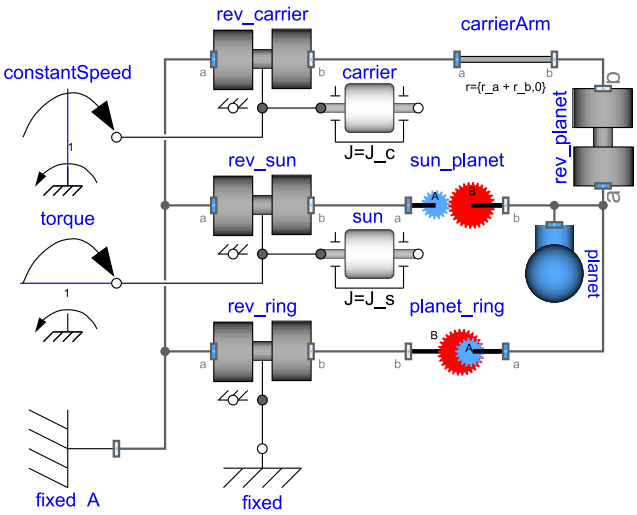

Figure 4. Modelica model of simple epicyclic gear configuration

2.5 Implementation of constraint equations

The gear model as depicted in Figure 2 needs a defined distance between point A and point B for a correct calculation of the forces and torques. However, when a constraint equation is defined in each gear contact model, epicyclic gear sets result in modeling problems since the planet–sun distances and sun–ring distance is defined double, thus leading to an overconstrained system. Therefore, these constraints cannot be defined in the model itself, but must be defined using the `PlanarMechanics` library. This mimics the behavior of real gears: a gear connection itself has no constraining equations. The gear wheel positions are defined by the bearing arrangement of the transmission.

An example of a simple epicyclic gear set is shown in Figure 4 and Figure 5. The structure of the model is similar to the gear construction. Hence, each bearing, mass and carrier is modeled in Modelica just like in a real system.

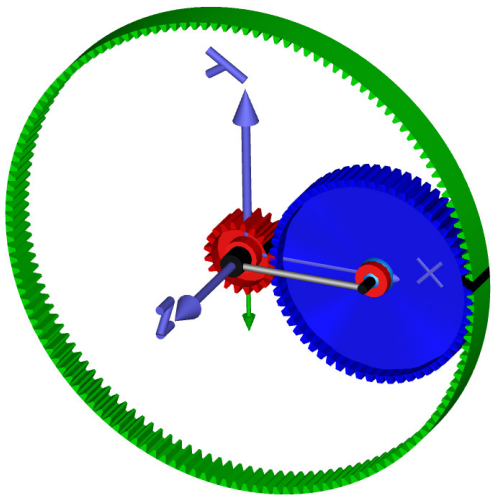

Figure 5. Graphical representation of the epicyclic gear configuration shown in Figure 4.

3 Construction of a torque vectoring drive in Modelica

The models as described in Section 2 are used to build a complete torque vectoring drive consisting of a Ravigneaux differential, superimposing gear and spur gear train.

3.1 Ravigneaux differential

The Ravigneaux differential is used to allow for different speeds of the car tires. Compared to common open differentials with bevel gears, using a Ravigneaux differential allows for a smaller construction envelope combined with lower losses. The Modelica representation of the differential is shown in Figure 6. The Ravigneaux differential uses four gear instances, together with a carrier which houses two connecting planets.

For simplicity reasons, only one set of planets is used in this analysis. When using all planet sets of a full Ravigneaux gear, the system would – in the case of rigid gear connections – lead to an overdetermined system. In the case of elastic gears, the different gear stages which can switch between friction modes can lead to heavy event chattering of the planets.

To compensate the stiffness reduction caused by the lower number of modeled planets, thicker gears with higher masses are incorporated.

The reduction of number of planets would lead to an unbalanced gear model as long as the masses of the planets are considered as well. But since the model in Figure 6 is purely rotationally coupled (see rotational flanges on both left and right side), this effect does not apply. On the contrary, if the bearing forces are studied, this planet number reduction will lead to wrong results. In this case, all planet masses should be added to balance the system and they must be rotationally coupled with the planet which is driven by the gear connections.

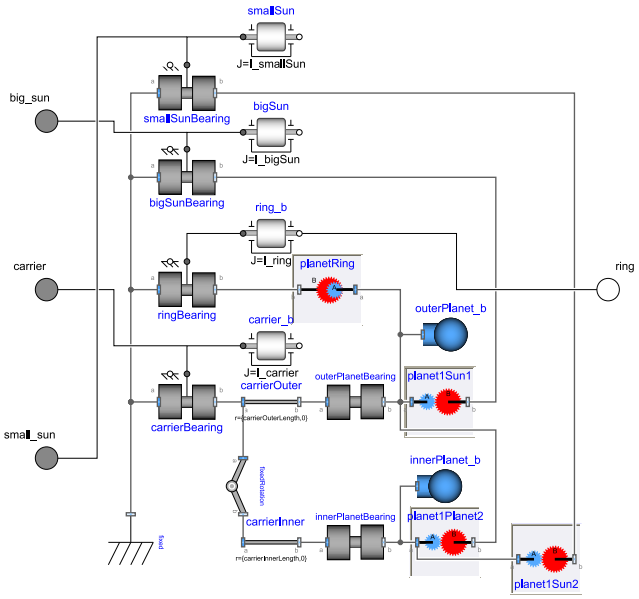

Figure 6. Ravigneaux differential

3.2 Superimposing gear

The superimposing gear uses the input torque to create a torque difference between the output flanges. Also in this case, only a single planet is modeled instead of all planets. The stiffness and mass are compensated to mimic all planets as depicted in Section 3.1. In Figure 7, the setup of the gear is shown. For the superimposing gear, four gear instances are needed.

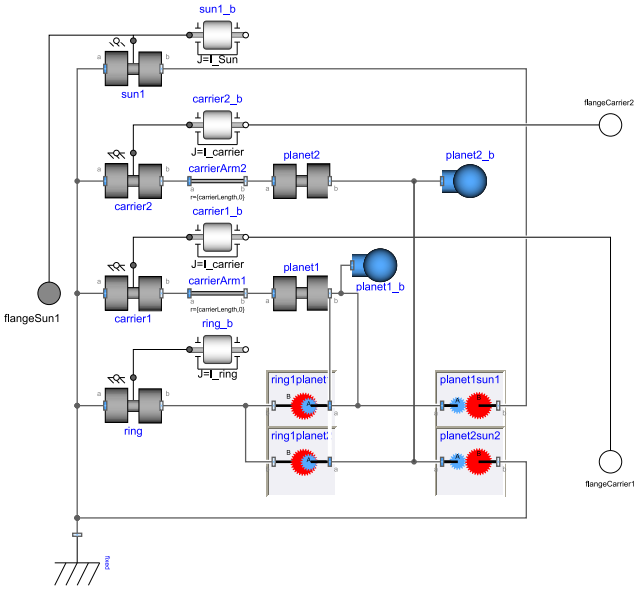

Figure 7. Superimposing gear

3.3 Overall TVD model

Connecting the Ravigneaux differential, superimposing gear and spur gear train together, a complete

DOI 10.3384/ecp15118151

Table 1. TVD model configurations under investigation

Configuration	Description
Fixed eta	Constant spring constant, constant gear efficiency
Fixed eta with Backlash	Nonlinear spring constant and backlash, constant gear efficiency
DIN 3990 eta with Backlash	Nonlinear spring constant and backlash, efficiency using to DIN 3990

TVD is generated as shown in Figure 8. To represent the connection elasticity between the drives, rotational stiffness-damping elements are added from the Modelica standard library.

In the overall TVD model, ten gear connections are included.

In the simulations which are presented in Section 5, three different configurations are analyzed according to Table 1.

The spring constant of the gear instances is set to 20×10^6 N/m/mm (Newton per meter per millimeter gear width), and the gear damping to 20×10^3 Ns/m/mm for all gear connections. The coupling between the superimposing gear, Ravigneaux gear and spur gear train have a stiffness of 10^7 Nm/rad and a damping of 10^5 Nms/rad, respectively.

4 Vehicle model

To analyze the TVD model in typical vehicle driving maneuvers, a vehicle model has to be utilized. For the sake of simplicity, a planar vehicle model was introduced which moves in the horizontal plane, thus enabling longitudinal, lateral and yaw motion only. Additionally, a six degrees of freedom mass (i. e. three positions and three rotations) was joined to the planar vehicle body. By taking into account the forces on this mass, wheel load variation due to vehicle mass transformation between wheels during braking, accelerating and cornering are enabled. The tire models allow slip and are based on the work of Zimmer and Otter (2010).

A small size electric vehicle with rear-wheel drive is considered for simulation. Its mass is about 1000 kg with wheelbase of 2.6 m and track of 1.45 m.

The powertrain of the vehicle consists of TVD as described above, the main motor which applies the main driving torque, and a differential motor which divides torques to the wheels of one axle. Utilizing the differential motor control, the torque vectoring functionality can be realized. Finally, driveshaft elements are considered as well to additionally incorporate their elasticity. An overview of the model is shown in Figure 9. To mimic the electrical time constant of the motors, a first order system with a time constant of 10^{-3} s for both motors is used.

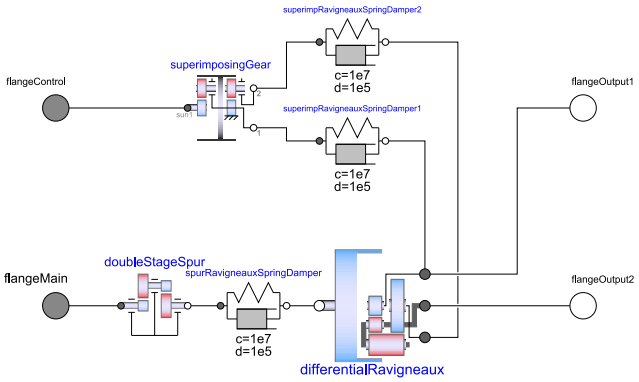

Figure 8. Complete TVD consisting of Ravigneaux differential, superimposing gear and spur gear train

5 Simulation results

Using the vehicle model with a free steering setup (free steering wheel), an acceleration maneuver is simulated. The main motor torque is given as a ramped signal, and the differential motor torque as a changing signal as shown in Figure 10.

5.1 Elastic drive shafts

The wheel torque of the right driveshaft during the maneuver is shown in Figure 11. It can be observed that the results of the constant efficiency and the DIN 3990 efficiency are differs significantly. The fixed efficiency cases (97% per gear stage) show a behavior which is intuitively expected of the TVD: the differential torque of the differential motor is amplified and split between the two axles.

Introducing the DIN 3990 friction model, the results yield – in contrast to the constant efficiency – an oscillating output torque. This is caused by the fact that due to the pre-load of the differential,

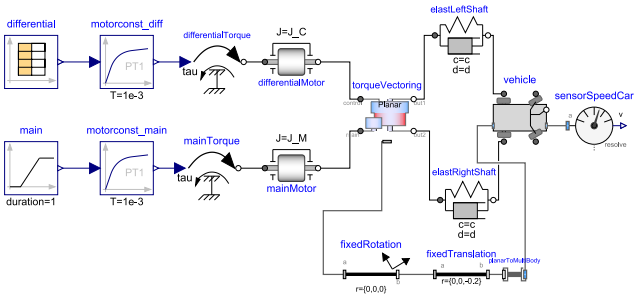

Figure 9. Vehicle model with motor configuration and driveshaft elasticity. The right bottom section of the diagram (with the planarToMultibody element) enables an animation where the drive is fixed to the car.

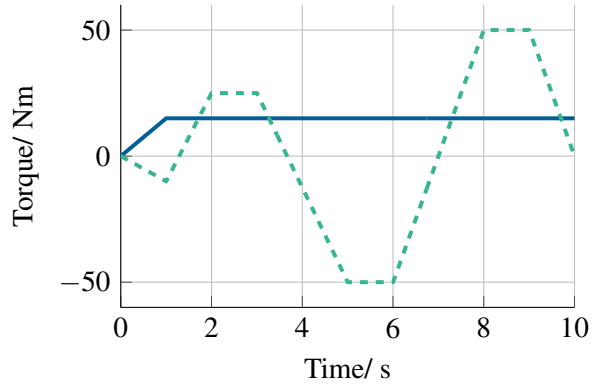

Figure 10. Motor torques during maneuver. The main motor toque (——) has a ramp of 1 s to 15 N m , the differential motor (- - -) is controlled with a changing reference torque.

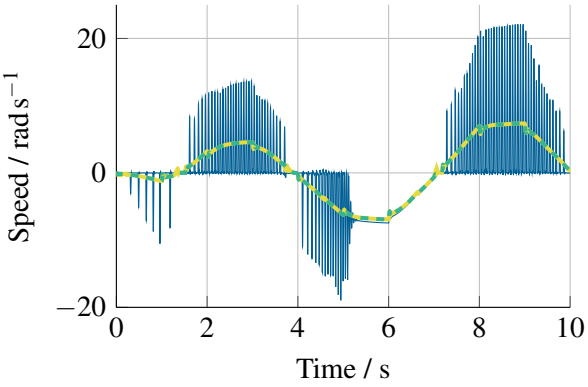

Figure 12. Speed of the differential motor using driveshafts with the reference stiffness. Different friction and elasticity models are shown: A fixed efficiency without backlash (- - -), fixed efficiency with backlash (——) and a friction law to the DIN 3990 standard (——).

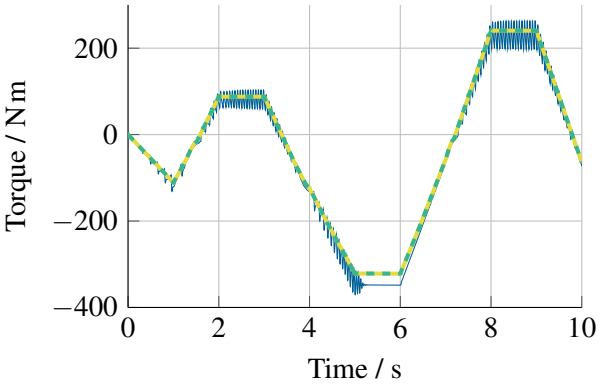

Figure 11. Wheel torques of the right driveshaft (reference stiffness) with different friction and elasticity models: A fixed efficiency without backlash (- - -), fixed efficiency with backlash (——) and a friction law to the DIN 3990 standard (——).

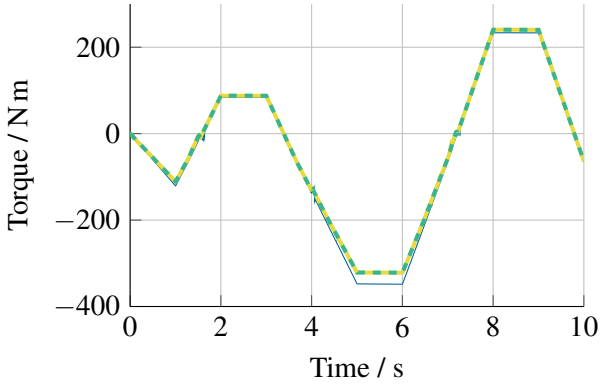

Figure 13. Wheel torques of the right driveshaft with different friction and elasticity models. A ten times increased stiffness of the driveshafts is used. A fixed efficiency without backlash (- - -), fixed efficiency with backlash (——) and a friction law to the DIN 3990 standard (——).

combined with low rotational velocities, lead to high friction. Due to this high friction combined with the pre-load, the gear can get in the stuck mode (this phenomenon is also described and measured for air path actuators by Ahmed et al. (2012)).

The combination of the drivetrain elasticity with high friction leads to a stick-slip problem resulting in highly varying torques. Note that without further measurements and / or experience on TVD, it cannot be concluded which of the friction models correctly represents the real system.

Analyzing the speed of the differential motor depicted in Figure 12, the stick-slip problem is also evident. High rotational accelerations are caused by the fast variation of the motor speed, which can lead to high loads on the rotor of the motor. This can lead to fatigue damage of the motor.

5.2 Stiff driveshafts

Using driveshafts with a significant higher stiffness and damping, the stick-slip problems described in Section 5.1 can be avoided. In presented example with increased stiffness, a ten times higher friction and damping has been used w.r.t. the nominal situation. The wheel torques of the right rear wheel (see Figure 13) behave as expected, also for TVD using the DIN 3990 friction model. Moreover, the high peaks in motor velocity of the differential gear are eliminated, cf. Figure 12 and Figure 14.

5.3 Simulation of eccentricities

Eccentricities are common in most gear wheels and are often caused by manufacturing tolerances. To simulate a non-perfect drive, an eccentricity of 10 µm is added to both gear wheels of the first stage of the spur gear train. This eccentricity excites the

DOI 10.3384/ecp15118151

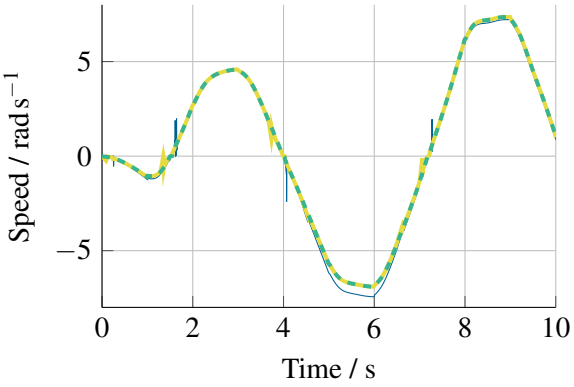

Figure 14. Speed of the differential motor using driveshafts with ten times increased stiffness. Different friction and elasticity models are shown: a fixed efficiency without backlash (- - -), fixed efficiency with backlash (——) and a friction law to the DIN 3990 standard (——).

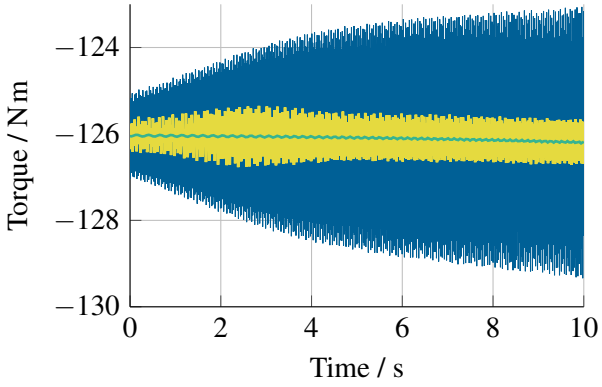

Figure 15. Wheel torques with and without gear eccentricities: All simulation results have a fixed efficiency and a nonlinear stiffness. The different lines show a simulation without eccentricity(——), simulation with the nominal stiffness (——) and a simulation with an increased stiffness(——).

gear train leading to vibrations. In this simulation, a constant torque of 5 N m is applied to the differential motor to keep the Ravigneaux differential out of the stuck mode. The main drive motor is driven with a constant load for a constant acceleration.

In Figure 15, the wheel torques of a simulation with a stiff driveshaft with eccentricity, an elastic driveshaft with eccentricity and an elastic driveshaft without eccentricity are given. Analyzing the simulation results, it is clear that this eccentricity has a high-frequent impact on the wheel torques. With a nominal driveline, the torque variations are lower at high velocities as for a stiff driveline. A detailed view of this vibration is shown in Figure 16. The high frequent vibrations of the gear seem to excite the drivetrain for the nominal stiffness drivetrain.

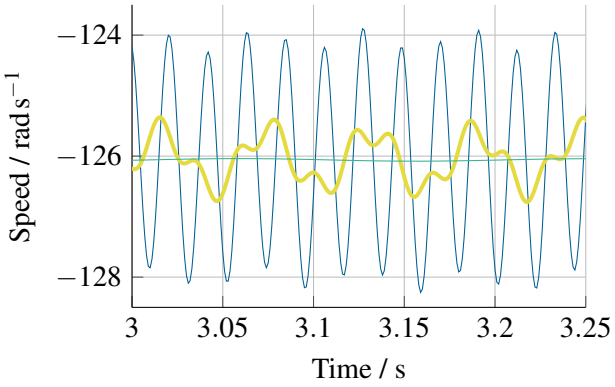

Figure 16. Speed of the differential motor with and without gear eccentricities: All simulation results have a fixed efficiency and a nonlinear stiffness. The different lines show a simulation without eccentricity(——), simulation with the nominal stiffness (——) and a simulation with an increased stiffness(——).

6 Discussion

During performed simulations, we realized that – due to the large number of switching components and high gear stiffness – the proposed model challenges common numerical solvers like DASSL or Radau IIA. Finding consistent restart conditions after an event can be hard, since this often directly triggers a next event in an adjacent gear connection.

In some cases, it is therefore advisable to use a regularized friction model as presented in Section 2.1. Such friction models can help to avoid events and make a simulation progress even if very complex gearing configurations are analyzed. However, most of these problems can be avoided by modeling the real-life world more accurately. As an example, in this paper, spring-damper models between the differential, superimposing gear and spur gear train have been added to mimic the stiffness of the connections. This avoided many problems with the simulation results.

7 Conclusion

In this paper, different techniques for gear modeling were presented and adopted for a torque vectoring drive which was analyzed in complete car model simulations. Applying such gear modeling techniques, which include losses, nonlinear elasticity and forcing errors, a various level of gear detail can be selected which proved to significant influence the simulation results.

The higher level of modeling detail is particularly important when investigating torque and speed oscillation issues which can be useful for e. g. driveline design. Then, simple fixed efficiency based friction models are insufficient. In contrast, DIN 3990 or

similar friction models are required to capture such effects. Furthermore, it was shown that both insufficient torsional stiffness of the drive shafts and stick slip in the gear lead to such large torque oscillations within a complete driveline.

The influence of gear eccentricities on the driveline was shown for driveshafts of different elasticity. It is shown that the a higher stiffness of this shaft increases the load on this axle. This shows that a trade-off must be made between the load caused by eccentricities and the load caused by the stick-slip effect, as a high driveshaft elasticity lowers the load caused by stick-slip effects, but increases the load caused by a stiffer shaft.

The drawback of some presented models can be an increased simulation effort due to large number of events. For such cases, the regularized friction model proved to be possible alternative.

It is worth mentioned that the model and the simulation results were not validated so far. Especially, the damping coefficient is largely unknown and not well researched at the moment. It is advisable to push the experimental research to get a usable estimate of the gear damping properties in the future.

References

F. S. Ahmed, S. Laghrouche, and M. El Bagdouri. Overview of the modelling techniques of actuator nonlinearities in the engine air path. *Proceedings of the Institution of Mechanical Engineers, Part D: Journal of Automobile Engineering*, 227(3):443–454, September 2012. ISSN 0954-4070. doi:10.1177/0954407012453905.

DIN 3990 Teil 4. Tragfähigkeitsberechnung von Stirnrädern; Berechnung der Freßtragfähigkeit, 1987.

Philipp Gwinner, Michael Otto, and Karsten Stahl. Lightweight Torque-Vectoring Transmission for the Electric Vehicle VISIO.M. In *COFAT 2014*, March 2014. URL `http://mediatum.ub.tum.de/doc/1226683/1226683.pdf`.

Gustav Niemann and Hans Winter. *Maschinenelemente: Band 2: Getriebe allgemein, Zahnradgetriebe - Grundlagen, Stirnradgetriebe (German Edition)*. Springer, 1989. ISBN 3-540-11149-2.

M Otter, H Elmqvist, and S E Mattsson. Hybrid modeling in Modelica based on the synchronous data flow principle. In *Computer Aided Control System Design, 1999. Proceedings of the 1999 IEEE International Symposium on*, pages 151–157, 1999. doi:10.1109/CACSD.1999.808640.

Franciscus L. J. van der Linden. Modelling of Elastic Gearboxes Using a Generalized Gear Contact Model. In *Proceedings of the 9th International MODELICA Conference*, pages 303–310, Munich, November 2012. Linkoping University Electronic Press. doi:10.3384/ecp12076303.

Franciscus L. J. van der Linden. Modeling of geared positioning systems: An object-oriented gear contact model with validation. *Proceedings of the Institution of Mechanical Engineers, Part C: Journal of Mechanical Engineering Science*, June 2015. ISSN 0954-4062. doi:10.1177/0954406215592056.

Dirk Zimmer. A Planar Mechanical Library for Teaching Modelica. In *Proceedings of the 9th International Modelica Conference*, pages 681–690, Munich, November 2012. Linköping University Electronic Press. doi:10.3384/ecp12076681.

Dirk Zimmer and Martin Otter. Real-time models for wheels and tyres in an object-oriented modelling framework. *Vehicle System Dynamics*, 48(2):189–216, February 2010. ISSN 0042-3114. doi:10.1080/00423110802687596. URL `http://www.tandfonline.com/doi/abs/10.1080/00423110802687596`.